



Politecnico di Bari

Repository Istituzionale dei Prodotti della Ricerca del Politecnico di Bari

Relationships between rain and displacements of an active earthflow: a data-driven approach by EPRMOGA

This is a post print of the following article

Original Citation:

Relationships between rain and displacements of an active earthflow: a data-driven approach by EPRMOGA / Vassallo, R.; Doglioni, Angelo; Grimaldi, G. M.; Di Maio, C.; Simeone, Vincenzo. - In: NATURAL HAZARDS. - ISSN 1573-0840. - STAMPA. - 81:3(2016), pp. 1467-1482. [10.1007/s11069-015-2140-9]

Availability:

This version is available at <http://hdl.handle.net/11589/60343> since: 2022-06-22

Published version

DOI:10.1007/s11069-015-2140-9

Publisher:

Terms of use:

(Article begins on next page)

Relationships between rain and displacements of an active earthflow: a data driven approach by EPRMOGA

R. Vassallo*, A. Doglioni**, G.M. Grimaldi*, C. Di Maio*, V. Simeone**

(* University of Basilicata, Italy)

(**) Technical University of Bari, Italy

Abstract

Inclinometer and piezometer measurements have been carried out since 2005 in a slow active earthflow in a clay shale formation of the Italian Southern Apennines. Previous studies outlined the main geometrical and kinematic features of the landslide and the pore pressure response to rainfall. Displacement rates seem to depend on the hydrological conditions as suggested by their seasonal variations. The availability of long time series of data, in some period recorded in *continuum*, allows the use of a data mining approach to evaluate the relations among displacement rates in different points of the landslide, and between displacement rates and rainfall. To define such relations, the evolutionary modelling technique EPRMOGA, based on a genetic algorithm, has been used in this paper. The results give a deeper insight into the landslide behaviour on one hand, and on the other show the reliability of the technique, also in building up management scenarios. In particular, they show that the landslide displacements in different points of the slip surface, characterized by different average velocities, are contemporary at the considered time resolution of 10 days. The obtained relations allow to quantify the displacement rate variations due to contemporary rainfall. The influence of past rainfall is shown to decrease exponentially with temporal distance. Furthermore, the EPRMOGA simulations seem to confirm that there are no other dominant causes, besides rainfall, responsible of displacement rate variations.

Keywords: landslide; displacement; rainfall; data driven model; EPRMOGA

1
2

1. Introduction

3 The displacement rates of active clayey landslides generally undergo seasonal
4 variations associated to hydrological conditions (Leroueil et al. 1996; Leroueil 2001
5 among others). To evaluate the relations among displacements, pore pressures and
6 rain, several different approaches are reported in the technical literature which can be
7 grouped into “physically based” and “phenomenologically based” (Cascini and Versace
8 1986). The former try to reproduce the physical processes of the system under study,
9 the latter aim finding empirical correlations between the landslide displacements and
10 their triggering factors, or statistical relationships between the measured groundwater
11 pressures and rainfall, without explicitly considering the physical processes occurring
12 in the slope.

13 Data-driven models are purely mathematical relationships among the variables of a
14 physical system which are not based on a physical analysis. They thus can be ascribed
15 to the group of “phenomenologically based” models. The types of input and output data
16 are obviously selected starting from a general physical knowledge of the phenomenon
17 under study, and the relationships among them are achieved by a trial and error
18 strategy or by an adaptive automatic procedure. Such models can suitably be applied
19 when long time series of monitoring data, such as inclinometer displacements,
20 piezometric levels and rainfall heights, are available.

21 In this paper, the data driven evolutionary modelling technique EPRMOGA (Giustolisi
22 and Savic 2009) is used to analyze the behaviour of the Costa della Gaveta earthflow,
23 a slow active landslide, up to about 40 m deep, developing in a structurally complex
24 clay shales formation of the Italian Southern Apennine. This earthflow is representative
25 of a landslide typology widely diffused in Italy and also in all the Mediterranean area
26 (Picarelli et al. 2000). Its displacements and pore pressures are being monitored since
27 2005 (Di Maio et al. 2010, Calcaterra et al. 2012, Vassallo et al. 2015), often with fixed
28 in place instruments—so that data driven analyses are possible. EPRMOGA already
29 proved effective to model the dynamics of environmental systems in several cases,
30 providing information on aquifer levels and landslide displacements (Doglioni et al.
31 2014; Doglioni et al. 2012; Doglioni et al. 2010; Giustolisi et al. 2008). The main
32 advantage of this procedure is that it provides closed-form equations, characterized by
33 relatively simple structures, that can be used both to forecast the landslide behaviour
34 and to obtain more information about the landslide through a physical interpretation of
35 the different terms of the equations.

36 For the case of Costa della Gaveta earthflow, the study has been carried out with the
37 two aims of verifying the capability of the proposed mathematical technique in the
38 evaluation of the relations among the involved physical parameters, for risk
39 management and forecasting purposes, and achieving a deeper insight in the
40 behaviour of an active clayey landslide. In particular, EPRMOGA has been used to
41 evaluate the correlations among the displacement rates in different boreholes, between
42 pore pressures and rainfall, and between displacements and rainfall. The absence of a
43 relation between displacements and pore pressures in single points has been justified
44 on the basis of previous studies (Vassallo et al., 2015) which show that the soil
45 properties and landslide geometry are such that the pore water response to rainfall is
46 characterised by noticeable depth-depending time lags. On the contrary, the
47 displacement rates determined by different inclinometers on the slip surface at different
48 depths are well correlated to one another and seem to depend on the overall pore water
49 response of the landslide.

1

2 **2. Costa della Gaveta landslide**

3 Costa della Gaveta landslide is an active slow earthflow of the Southern Italian
4 Apennines. It is about 1250 m long, from 100 to 600 m wide, with an average inclination
5 of about 10° (Fig. 1). It is characterized by a maximum depth of about 40 m, a wide
6 source area, mostly emptied, a straight channel and a large accumulation area. The
7 material in the channel moves slowly or extremely slowly (Cruden and Varnes 1996),
8 with displacement rates decreasing in the downslope direction.

9 The landslide occurs in two different geological formations: Varicoloured Clays and
10 Corleto Perticara. Varicoloured Clays are constituted by an irregular alternation of thin
11 beds of clays, marly clays and clayey marls. Corleto Perticara formation is constituted
12 by an irregular succession of calcareous marls, marly limestones, white-grey calcilutites
13 and, in the Costa della Gaveta zone, by frequent grey-brown clay layers up to about
14 some meters thick.

15 The earthflow body, mainly constituted by destructured clays with abundant rock
16 fragments, rather inhomogeneous, is characterized by a clay fraction *c.f.* up to 50% and
17 liquid limit w_L between 40% and 80%. Below the first 2 m, the degree of saturation S_r
18 can be considered equal to 100 %. An average residual friction angle ϕ'_r of about 10°
19 was determined by laboratory tests (Di Maio et al. 2013, Di Maio et al. 2015).

20 Displacements are being monitored since 2005 in several verticals by inclinometers
21 (Fig. 1) and a long rainfall time series is available. Pore pressures measurements are
22 also available. Periods and frequency of measurement, and instrument accuracy, are
23 reported in Table 1.

24 Displacement profiles have been obtained by frequent inclinometer measurements
25 during the 10 years monitoring. A slip surface with a depth up to 40 m in the transition
26 zone between the channel and the accumulation zone was detected (Fig. 2). In some
27 boreholes, once the depth of the slip surface had been detected, fixed-in-place
28 inclinometer probes with continuous data acquisition were installed.

29 Along the slip surface, the displacements occur with very different rates, decreasing in
30 the downslope direction (Fig.3a), however they seem to be strongly correlated to each
31 other in the whole monitoring period. Di Maio et al. (2010) and Di Maio et al. (2013)
32 showed that such correlation is justified by a mechanism of constant soil discharge
33 through the landslide channel. In fact, during the monitoring period, the same soil
34 discharge (estimated by displacement rates and landslide cross section areas) is
35 observed in different cross sections at the same time. The correlation can be better
36 appreciated in Fig. 3b in which all the time series overlap by simply dividing each of
37 them by a constant. Fig. 4 reports the displacement rates (divided by the same
38 constants as in Fig. 3b), which for I9, I9b and I12 were also evaluated by fixed-in-place
39 inclinometer measurements over about two years. Such rates, evaluated as 15 days-
40 moving averages, agree with those of periodical manual measurements. The figure
41 shows seasonal variations which can be reasonably attributed to the hydrological
42 regime of the site.

43 The hydrological regime of the area is characterized by rainfalls of long duration and
44 low medium intensity; short rainfalls of high intensity are quite rare. As typical of Italian
45 peninsula, more than 60% of the total yearly rain falls during autumn and winter. The
46 long historical rainfall series is characterized by a substantial uniformity over the years,
47 as shown by Fig. 5a which reports the yearly cumulative rainfall from 1980 to 2015. The

1 rainfall relative to the monitoring period (2005-2015) can be considered representative
2 of the longer period (Fig. 5b).

3 Pore pressures were monitored by means of some electric and Casagrande
4 piezometers at 15 m and 30 m depths, whose location is shown in Fig.1. The
5 Casagrande piezometers were also used for the evaluation of the hydraulic conductivity
6 k of the different formations of the subsoil (Fig.1). By falling head tests, values of k in
7 the range 10^{-9} m/s - 10^{-8} m/s were evaluated in the landslide body, about 10^{-10} m/s in
8 the stable Varicoloured Clays, and 10^{-7} m/s in the Corleto Perticara formation. Vassallo
9 et al. (2015) reported the results of a transient simulation, by the 3D finite difference
10 code MODFLOW, of pore pressure response to a historical rainfall. A simulation with
11 daily resolution succeeded in reproducing accurately an electrical piezometer data (S3,
12 whose position is shown in Fig. 1) over the two years of continuous monitoring. The
13 results of such analysis were thus used to interpret the landslide pore water pressure
14 response to rainfall. The results show that: i) the response to rain along the slip surface
15 is characterised by noticeable depth-depending time lags, and ii) pore water pressure
16 variations induced by rainfall are significant only at depths lower than about 10 m. On
17 the other hand, the displacement rates determined by different inclinometers on the slip
18 surface are well correlated to one another: the landslide apparently moves with a
19 constant soil discharge in the channel (Di Maio et al. 2010), whose trend seems very
20 close to that of the average pore water pressure on the slip surface. The displacement
21 rates on the slip surface are thus not correlated to pore water pressures in single points,
22 i.e. to any single piezometer data.

23

24 **3. EPRMOGA: assumptions and procedures**

25 The availability of long time series of displacements, pore pressures and rainfall allows
26 the use of the EPRMOGA data mining approach. This technique is a data-driven multi-
27 objective evolutionary modelling technique (Giustolisi and Savic 2009), which proves
28 particularly effective at modelling environmental phenomena characterized by high
29 non-linearity, even with poor *a-priori* knowledge about their dynamics (Doglioni and
30 Simeone 2014). It does not require pre-assumed equations governing the phenomenon
31 under investigation. It does not need the calibration of physical parameters, and is
32 particularly serviceable for managing purposes. Furthermore, a critical analysis of the
33 relationships provided by EPRMOGA between input and output data can give an insight
34 into the physics of the system even in the case of nonlinear processes.

35 The procedure is composed of two stages: a) identification of the model structure based
36 on a genetic algorithm (Goldberg 1989; Giustolisi et al. 2004), b) estimation of the
37 coefficients, based on a least-square approach. Assumptions are done on: structures
38 of the equations, potentially involved functions, maximum length of the polynomial,
39 exponents and objective functions, so as to set a limit to the evolutionary search, i.e. to
40 the space of solutions. During the search for the equations, EPRMOGA can
41 simultaneously minimize: a) the sum of squared errors, b) the number of terms, and c)
42 the number of input variables. In this sense the approach is multi-objective, as three
43 conflicting functions are simultaneously optimized. This allows to optimize the fit of the
44 model to input data and to obtain simple structures that can be potentially interpreted.
45 As a result, a set of solutions is provided, known as Pareto set (Pareto, 1896), which
46 represents the trade-off among the three objective functions. None of the solutions can
47 thus be considered the best among the others. In this way, EPRMOGA allows to
48 compare the equations of the Pareto set and then to make a more robust choice of the

1 equation, on the basis of both structure and involved variables. The choice is based on
2 a compromise between the fit to experimental data and the structural parsimony of
3 equations allowing a physical interpretation of the terms.

4 In this study, EPRMOGA is used to evaluate the correlation:

5 a) among the displacement rates in different boreholes;

6 b) between pore pressures and rainfall;

7 c) between displacements and rainfall.

8 EPRMOGA did not find direct relations between displacements and pore pressures
9 measured at a specific depth, consistently with the results of Vassallo et al. (2015)
10 recalled in the previous section.

11 Used input data are: average deep displacement rates over 10 days intervals, pressure
12 head values extracted from the data series every 10 days, and cumulative rainfall
13 heights over 10 days. This time interval allows a quite good resolution and a sufficient
14 numerosity of data series. Given the very low displacement rates, a higher time
15 resolution would be much affected by measurement uncertainty.

16 The model structure is assumed to be polynomial and the variables involved by each
17 term, as well as the number of terms, are identified by EPRMOGA. Only positive terms
18 have been considered since negative ones, for the studied phenomenon, would be
19 purely interpolative, without physical soundness. Values of the variables at several
20 different times can be assigned as input to the models. For example, in the analysis of
21 the relations displacement rates vs. rainfall, the assumed candidate pool of variables
22 includes: v_{t-1} and v_{t-2} , i.e. displacement rates at 10 days and 20 days before the output,
23 and $P_t, P_{t-1}, P_{t-2}, P_{t-3}, P_{t-4}, P_{t-5}, P_{t-6}$, i.e. rainfall ranging from contemporary to 60 days
24 before. To limit the complexity of the models, the exponents of the variables are
25 assumed to be either 0, 1 (linear relationship), 0.5 (attenuation) or 2 (amplification).
26 Each provided model is the outcome of an optimization aimed at the structural
27 parsimony as well as at the maximization of the fitness to measured data. This is why
28 not all the variables are expected to appear in the models.

29 Similarly, as far as the relationship pore pressures vs. rainfall is concerned, variables
30 include u_{t-1} and u_{t-2} , i.e. pore pressures at 10 and 20 days before the output, and rainfall
31 $P_t, P_{t-1}, P_{t-2}, P_{t-3}, P_{t-4}, P_{t-5}, P_{t-6}$ from contemporary to 60 days before.

32 The fitness of model output to measured data is evaluated by the Coefficient of
33 Determination (CoD):

$$34 \quad CoD = 1 - \frac{N-1}{N} \frac{\sum_N (v_{EPR} - v_{exp})^2}{\sum_N [v_{exp} - avg(v_{exp})]^2} \quad (1)$$

35

1 where N is the number of samples, v_{EPR} and v_{exp} are displacement rates, respectively
2 returned by EPRMOGA and measured, and $avg(v_{exp})$ is the average of v_{exp} values. The
3 closer to 1 is the CoD, the better is the model simulation of measured data.

4 The comparison of the models obtained by EPRMOGA and the experimental data can
5 be carried out in two different ways, to predict displacements or pore pressures over
6 the whole studied period (this mode is called “simulation” in the following), or over only
7 some time steps ahead (this mode is called “prediction” in the following). In the
8 simulation over the whole period of interest, once the initial condition is defined, the
9 past values of displacement rate or pore pressure are recursively estimated by the
10 model itself. In other words, given the rainfall values, the model becomes completely
11 determined. Differently, in the prediction over a shorter period, the estimation of the
12 previous values by the model is periodically substituted by the experimental data. Thus
13 the model is periodically set out to reality. If the results of simulation agree with those
14 of measurements, then the general behaviour of the system was caught. The difference
15 between measured and calculated values may be locally different for several reasons,
16 but if measured and simulated values do not diverge in the long period it means that
17 the model is able to simulate the system general behaviour. Local differences may be
18 due to several reason, such as measurement errors or influence of extra-input not
19 considered in the analysis.

20

21 **4. EPRMOGA: results**

22 The EPRMOGA equations of displacement rates have been evaluated for inclinometers
23 I9b and I9c, located in the same transversal section of the channel, and I12, located at
24 the head of the landslide body (Figs. 1 and 2) because of the availability, in such
25 verticals, of continuous data for some years and for their higher velocity. The location
26 of inclinometers I9b and I9c was chosen so as to study the velocity distribution in
27 ~~deformation of~~ a transversal section. Inclinometer measurements in I7, in the lower part
28 of the landslide, have not been used due to the very low velocities (about 1 mm/year).
29 Data relative to I8, recorded with lower frequency by manual measurements (Tab. 1),
30 have not been used to determine a model but have been analyzed by the equations
31 found for the other boreholes.

32 For pore pressures analyses, the results relative to the electric piezometer S3 with
33 continuous data acquisition will be used. Such piezometer is located in the nearby
34 Varco D’Izzo landslide (Fig. 1), which develops in the same materials as Costa della
35 Gaveta landslide, and is the only electric piezometer in the studied zone which provided
36 continuous data for a period of two years without interruptions. Vassallo et al. (2015)
37 showed that its data can be considered representative of the pore pressure response
38 in Costa della Gaveta. They also reported measurements of the electric piezometer S9
39 located in Costa della Gaveta landside (Fig. 1) showing that, in the few months in which
40 it was in use, it provided pressure values comparable to those measured by S3 at the
41 same depth.

1 For each analysis, a Pareto set of equations is identified. Then, among these, one
2 equation will be chosen, according to the above mentioned criterions.

3

4 4.1 Relationships among displacement rates of inclinometers located in different 5 positions of the landslide profile

6 The analysis has been performed over the period November 2012 - May 2015 during
7 which data have been obtained by fixed in place probes. Data obtained before then
8 have not been used since manual inclinometer measurements had been carried out
9 with a frequency lower than that required by the analysis, that is 1/10days.

10 The relationships among the deep displacement rates in I9b, I9c, and I12 has been
11 sought, for each couple of inclinometers, also switching the dependent and
12 independent variables. The selected equations, plotted in Figs. 6-8, are the following:

$$13 \quad v_t^{I9b} = 0.243v_t^{I12} + (0.010 \text{ cm/10days}) \quad (2)$$

$$14 \quad v_t^{I12} = 2.692v_t^{I9b} \quad (2')$$

$$15 \quad v_t^{I9b} = 0.849v_t^{I9c} + (0.011 \text{ cm/10days}) \quad (3)$$

$$16 \quad v_t^{I9c} = 0.723v_t^{I9b} \quad (3')$$

$$17 \quad v_t^{I9c} = 0.220v_t^{I12} + (0.004 \text{ cm/10days}) \quad (4)$$

$$18 \quad v_t^{I12} = 1.793 \cdot \sqrt{v_{t-1}^{I12} \cdot v_t^{I9c}} + (0.007 \text{ cm/10days}) \quad (4')$$

19 Figs. 6, 7 and 8, that compare experimental data to those simulated by the above
20 equations, show a satisfactory model performance. CoD values, reported in the figures,
21 confirm that equations (2) and (2') provide a good agreement between measured and
22 model-returned displacement rates. Equations (3), (3') and (4) have still a rather good
23 performance. The correlation becomes worse for eq. (4') (I12 vs I9c) but is still able to
24 reproduce the general behaviour of I12. For each couple of equations, the first one
25 does not correspond to the second one inverted because it was *a priori* assumed that
26 all the coefficients are positive.

27 With the exception of (4'), the equations relate contemporary displacement rates only,
28 thus suggesting the simultaneity, under the considered time resolution, of
29 displacements in correspondence of the different points of the landslide slip surface.
30 Thus there seems to be no delayed propagation phenomenon appreciable at the used
31 time scale. This agrees with the observation that the displacements of the different parts
32 of the landslide are strongly correlated to one another as an effect of a constant soil
33 discharge mechanism of movement in the channel (Di Maio et al. 2010). Furthermore,

1 it can be observed that five out of six equations are linear and provide ratios between
2 the velocities very close to those reported in Figs. 3b and 4.

3 It is worth noting that, with the exception of eq. (4'), the models do not contain the term
4 of displacement rate at the previous time steps, thus EPRMOGA works just in
5 simulation mode all over the considered period.

6

7 *4.2. Relationships between pore pressures and rainfall*

8 Pressure head (u/γ_w) variations recorded continuously by piezometer S3 (Fig. 1, Tab.
9 1) from 2005 to 2008 have been here analysed as a function of rainfall. The best fitting
10 equation provided by EPRMOGA is:

$$11 \left(\frac{u}{\gamma_w} \right)_t = 0.0584 P_t^{0.5} + 0.032 \left(\frac{u}{\gamma_w} \right)_{t-1}^2 + 7.233 \quad (5)$$

12 with u/γ_w in m and rainfall in mm.

13 The equation is very simple and has a quite satisfactory performance in the simulation
14 mode (Fig. 9). The first term of the equation, damped by the exponent 0.5, is
15 representative of the response to contemporary rainfall. The second one is a “memory
16 term” representative of the effect of the state of the system as determined by previous
17 rainfall. The third term probably contains the effect of hydraulic conditions on
18 boundaries different from the ground surface.

19 It is interesting to observe that the behaviour described by eq. (5) is very similar to that
20 obtained by Vassallo et al. (2015), for the same piezometer, through the physically
21 based Modflow 3D simulation. So the results of the two models, obtained using different
22 approaches, are in good agreement, as clearly shown by Fig. 9, and very close to the
23 experimental data.

24 Pore pressures measured by Casagrande piezometers were also used to evaluate the
25 relationship between pressure head and rainfall. However, EPRMOGA did not find any
26 relation. This agrees with the results of Vassallo et al. (2015) who showed that the
27 Casagrande piezometers' data are characterized by noticeable time lag and lower
28 sensitivity to individual rainfalls than the electric piezometer S3.

29

30 *4.3. Relationships between displacement rates and rainfall*

31 EPRMOGA returned equations of displacement rates vs. rainfall similar for the different
32 inclinometers:

$$33 v_t^{I12} = 0.000787 \cdot P_t + 0.707 \cdot v_{t-1}^{I12} \quad (6)$$

$$1 \quad v_t^{I9b} = 2.590 \cdot 10^{-6} \cdot P_t^2 + 0.718 \cdot v_{t-1}^{I9b} + 0.004 \quad (7)$$

$$2 \quad v_t^{I9c} = 2.453 \cdot 10^{-6} \cdot P_t^2 + 0.689 \cdot v_{t-1}^{I9c} + 0.002 \quad (8)$$

3 with displacement rates in cm/10days and rainfall in mm.

4 Figures 10, 11 and 12 report displacement rates evaluated over the whole considered
5 period (November 2012 – June 2015), and of 40-days-ahead predictions, showing that
6 there is no substantial improvement in the prediction compared to the simulation. The
7 agreement with experimental data, with CoD ranging from 0.59 to 0.73, can be
8 considered satisfactory.

9 The equations include a term of persistence, i.e. the velocity at the previous time step,
10 that has an influence of about 70%, a term related to contemporary rainfall and a third
11 term, constant, whose value is very close to zero. The above equations also imply that,
12 in dry periods ($P=0$), displacement rate decreases by about 70% per time step, i.e.
13 exponentially.

14 It is interesting to analyze in detail the persistence term. For example, eq. (6) can be
15 re-written as:

$$16 \quad v_t = a \cdot P_t + 0.71v_{t-1} \quad (6')$$

17 and, applied in sequence for successive time steps, it becomes:

$$18 \quad v_t = a \cdot P_t + 0.71 \cdot (aP_{t-1} + 0.71v_{t-2}) = a \cdot [P_t + 0.71P_{t-1} + 0.71 \cdot (aP_{t-2} + 0.71v_{t-3})] =$$

$$19 \quad = a \left(\sum_{i=0}^{n-1} 0.71^i P_{t-i} \dots \right) + 0.71^n v_{t-n} \quad (6'')$$

20 which can be approximated by neglecting the last term and considering just a few P_{t-i}
21 terms. For example, by considering 7 terms we obtain:

$$22 \quad v_t \cong a \cdot (P_t + 0.71P_{t-1} + 0.71^2 P_{t-2} + 0.71^3 P_{t-3} + 0.71^4 P_{t-4} + 0.71^5 P_{t-5} + 0.71^6 P_{t-6}) \quad (6''')$$

23 which explicitly expresses the dependency of displacement rate on past rainfall. Fig. 13
24 shows that even just the first 5 terms of eq. (6'') reproduce very accurately the trend of
25 eq. (6).

26 Equation (6), which relates the displacement rate of I12 (installed in august 2012) to
27 rainfall, calibrated in the period 2013-2015, was used to evaluate the displacements
28 which could have occurred in the same location in the eight years before (2005-2013)
29 during which other inclinometers were in use. Fig. 14 shows that the calculated values
30 of I12 agree with the experimental data of the other inclinometers (I10, I9, I8) if each
31 data series is multiplied by a constant. The used values of constants are the same as
32 those reported in Fig. 4. Among other things, this suggests that there are not other

1 dominant causes, besides rainfall, responsible of the landslide displacement rate
2 variations. It seems thus reasonable to hypothesize that, in the absence of exceptional
3 events, natural or anthropic, and for an unchanged hydrological regime, the next future
4 behaviour of the landslide will not be different from the current one. Actually, on the
5 basis of incoming climate changes, a modest decrease in the piezometric levels, and
6 thus a decrease in the annual displacement, was hypothesized by Comegna et al.
7 (2013). The Authors examined the potential changes in the pore water pressure of
8 Costa della Gaveta slope in the next 50 years. For an inclinometer in the nearby Varco
9 d'Izzo landslide (I3 in Fig.1), comparable to I12 for displacement rates and slip surface
10 depth, they evaluated an average decrease between 1.5 and 3 mm/decade per
11 decade, depending on the climate scenario, with phases of moderate acceleration
12 during winter and spring. The rate decrease is negligible, since a substantially linear
13 trend in average yearly cumulative displacements was obtained.

14

15 **5. CONCLUSIONS**

16 The Costa della Gaveta earthflow is a slow active landslide which occurs in a
17 structurally complex clay shales formation of the Italian Southern Apennine. Its
18 displacements and pore pressures are being monitored since 2005, often with fixed in
19 place instruments. In this paper, the relationships among displacements, pore
20 pressures and rainfall has been sought through an evolutionary modelling data driven
21 technique called EPRMOGA, based on a genetic algorithm. Its main advantage is that
22 it provides closed-form equations, with the different terms characterized by relatively
23 simple structures, so that the physical interpretation of the phenomenon under
24 examination can be attempted.

25 The study has allowed to achieve a deeper insight in the behaviour of a widely diffused
26 type of landslide.

27 The results show that the landslide displacements in different points of the slip surface
28 are contemporary at the considered time resolution (10 days), consistently with the
29 hypothesis by Di Maio et al. (2010) of constant soil discharge in the landslide channel.
30 The relation found between pore pressures and rainfall is able to reproduce quite
31 accurately the experimental data and also the results of a physically based 3D model
32 (MODFLOW). The obtained relations allow to quantify the displacement rate variations
33 due to contemporary rainfall and the influence of past rainfall, which decreases
34 exponentially with temporal distance. Furthermore, EPRMOGA simulations suggest
35 that there are no other dominant causes, besides rainfall, responsible of the landslide
36 displacement rate variations.

37 Finally, the study has shown the reliability of EPRMOGA in the evaluation of the
38 relations among the physical parameters involved in the behaviour of active landslides
39 belonging to the same typology of the considered one, even for management and
40 forecasting purposes.

41

42 **ACKNOWLEDGEMENTS**

1 Part of this research has been funded by the Italian Ministry of Instruction, University
2 and Research (PRIN project 2010–2011: landslide risk mitigation through sustainable
3 countermeasures).

4

5 REFERENCES

- 6 Calcaterra S., Cesi C., Di Maio C., Gambino P., Merli K., Vallario M., Vassallo R. (2012).
7 Surface displacements of two landslides evaluated by GPS and inclinometer systems: a case
8 study in Southern Apennines, Italy. *Natural Hazards*, 61, 257-266.
- 9 Cascini L., Versace P. (1986). Eventi pluviometrici e movimenti franosi. Proceedings XVI Italian
10 Geotechnical Conference, 14-16 May, Bologna, Italy, Vol. 3, 171-184.
- 11 Comegna L., Picarelli L., Bucchignani E., Mercogliano P. (2013). Potential effects of incoming
12 climate changes on the behaviour of slow active landslides in clay. *Landslides* 10, 373-391.
13 DOI 10.1007/s10346-012-0339-3.
- 14 Cruden D.M., Varnes D.J. (1996). Landslide types and processes, in: *Landslide: Investigation
15 and Mitigation*. Special Report 247. Transportation Research Board, Washington, 36–75.
- 16 Di Maio C., Vassallo R., Vallario M., Pascale S., Sdao F. (2010). Structure and kinematics of a
17 landslide in a complex clayey formation of the Italian Southern Apennines. *Engineering
18 Geology*, vol. 116, pp. 311-322.
- 19 Di Maio C., Vassallo R., Vallario M. (2013). Plastic and viscous displacements of a deep and
20 very slow landslide in stiff clay formation. *Engineering Geology*, 162, 53-66.
- 21 Di Maio C., Scaringi G., Vassallo R. (2015). Residual strength and creep behaviour on the slip
22 surface of specimens of a landslide in marine origin clay shales: influence of pore fluid
23 composition. *Landslides*, 12, 657–667, DOI 10.1007/s10346-014-0511-z
- 24 Doglioni A., Mancarella D., Simeone V., Giustolisi O. (2010). Inferring groundwater system
25 dynamics from time series data, *Hydrological Sciences Journal*, IAHS press, 55 (4) 593-608 -
26 ISSN 0262-6667.
- 27 Doglioni A., Fiorillo F., Guadagno F.M., Simeone V. (2012). Evolutionary polynomial regression
28 applied to rainfall triggered landslide reactivation alert, *Landslides*, Springer, 9(1), 53-62, DOI:
29 10.1007/s10346-011-0274-8; ISSN: 1612-510X.
- 30 Doglioni A., Simeone V. (2014). Data-driven modeling of the dynamic response of a large deep
31 karst aquifer. *Engineering Procedia*, 89(C), 1254-1259; 16th Conference on Water Distribution
32 System Analysis, WDSA 2014 – Bari (Italy), July 2014. doi: 10.1016/j.proeng.2014.11.430.
- 33 Doglioni A., Galeandro A., Simeone V. (2014) Evolutionary data-driven modeling of Salento
34 shallow aquifer response to rainfall. *Engineering Geology for Society and Territory – Volume 3
35 River Basins, Reservoir Sedimentation and Water Resources (IAEG XII Congress, September
36 15-19, 2014, Torino, Italy)* Eds: Lollino G., Arattano M., Rinaldi M., Giustolisi O., Marechal J.C.,
37 Grant G.E. ISBN: 978-3-319-09053-5; doi: 10.1007/978-3-319-09054-2_58.
- 38 Giustolisi O., Doglioni A., Laucelli D., Savic D.A. (2004). A proposal for an effective
39 multiobjective non-dominated genetic algorithm: the OPTimised Multi-Objective Genetic
40 Algorithm, OPTIMOGA. Report 2004/07, School of Engineering Computer Science and
41 Mathematics, Centre for Water Systems, University of Exeter, UK.
- 42 Giustolisi O., Doglioni A., Savic D.A., di Pierro F. (2008). An Evolutionary Multi-Objective
43 Strategy for the Effective Management of Groundwater Resources, *Water Resources
44 Research*, 44, W01403. doi: 10.1029/2006WR005359.
- 45 Giustolisi O., Savic D.A. (2009). Advances in data-driven analyses and modelling using EPR-
46 MOGA. *Journal of Hydroinformatics*, 11(3–4): 225–236.

- 1 Goldberg D.E. (1989). Genetic Algorithms in Search, Optimization, and Machine Learning.
2 Addison Wesley, 432 p.
- 3 Leroueil S. (2001). Natural slopes and cuts: movement and failure mechanisms. *Géotechnique*,
4 51(3), 197 –243.
- 5 Leroueil S., Locat J., Vaunat J., Picarelli L., Lee H., Faure R. (1996). Geotechnical
6 characterization of slope movements. Proceedings of the VII international Symposium on
7 Landslides, Trondheim, 1, 53 – 74.
- 8 Pareto V. (1896). *Cours D'Economie Politique*. Rouge and Cic, Vol. I and II, Lausanne,
9 Switzerland.
- 10 Picarelli, L., Olivares, L., Di Maio, C., Urciuoli, G. (2000). Properties and behaviour of tectonized
11 clay shales in Italy. Proceedings of the II International Symposium on Hard Soils and Soft
12 Rocks, Napoli, Italy 1998, pp. 1211–1242 (Rotterdam, Balkema).
- 13 Vassallo R., Grimaldi G.M., Di Maio C. (2015). Pore pressures induced by historical rain series
14 in a deep-seated clayey landslide: 3D modeling. *Landslides*, 12, 731–744, DOI
15 10.1007/s10346-014-0508-7.

Table 1. Type, periods and frequency of measurements. Instrument accuracy is: $\pm 6\text{mm}/25\text{m}$ for manual inclinometer probe; $\pm 15\text{mm}/25\text{m}$ for fixed in place probe; $\pm 2\text{ kPa}$ for electric piezometer. Manual inclinometer measurements were performed at 0.5 m intervals by a 0.5 m long probe. In correspondence of the slip surface, some measurements were carried out 10 cm intervals. Inclinometer measurements were validated by spiral correction and by performing periodical measurements in all the grooves (“A” and “B”) of the inclinometer casings. Azimuth was always checked. First months of measurements were excluded from results.

Inclinometer	Type of measurement	Operational period	Reading frequency (t⁻¹)	Cause of interruption
I8	manual	Mar 2005 – Nov 2013	1/(1 month)	inclinometer tube sheared off
I9	manual	Mar 2005 - Jul 2006 ----- Feb 2010 - Feb 2012	1/(1 month) ----- 1/(1 month)	installation of fixed in place probe ----- inclinometer tube sheared off
	fixed in place probe	Jul 2006 – Jan 2009	1/(2 hrs)	electric malfunctioning probably due to corrosion of cables
I10	manual	Mar 2005 – Dec 2007	1/(1 month)	inclinometer tube sheared off
I9b	manual	Mar 2012 – May 2014	1/(1-2 weeks)	installation of fixed in place probe
	fixed in place probe	May 2014 - present	1/(2 hrs)	-
I9c	manual	Jan 2013 - present	1/(1-2 weeks)	-
I12	manual	Jul 2012 - Feb 2014	1/(1-2 weeks)	installation of fixed in place probe
	fixed in place probe	Feb 2014 – present	1/(2 hrs)	-
Piezometer	Type of measurement	Operational period	Reading frequency	Cause of interruption
S3 (depth: 14.5 m)	electric	Mar 2005 – Oct 2008	1/(2 hrs)	electric malfunctioning probably due to corrosion of cables

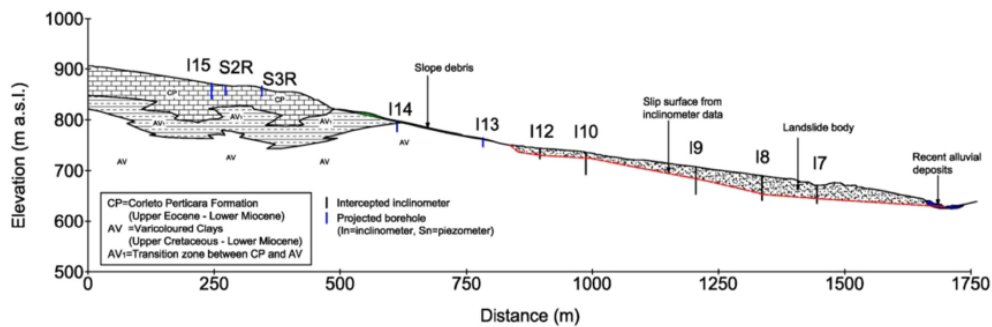
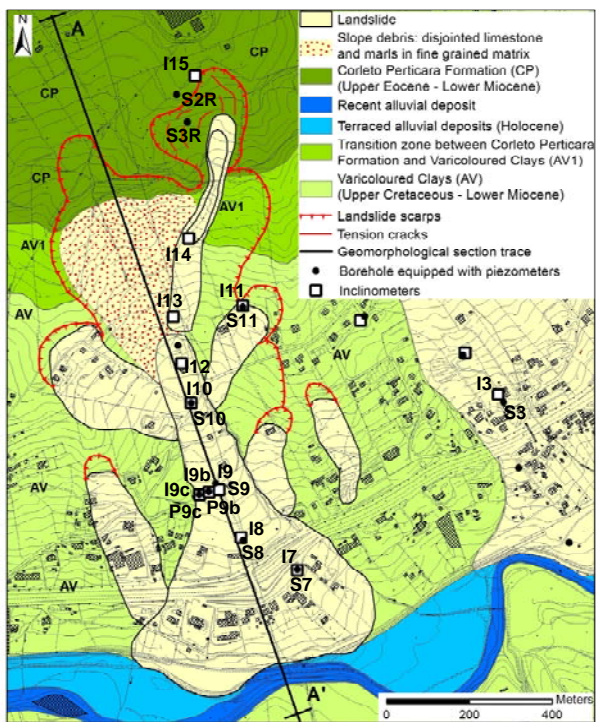


Fig. 1. Costa della Gaveta landslide with the localization of piezometers (S, P) and inclinometer casings (I): geological map and section (after Vassallo et al. 2014).

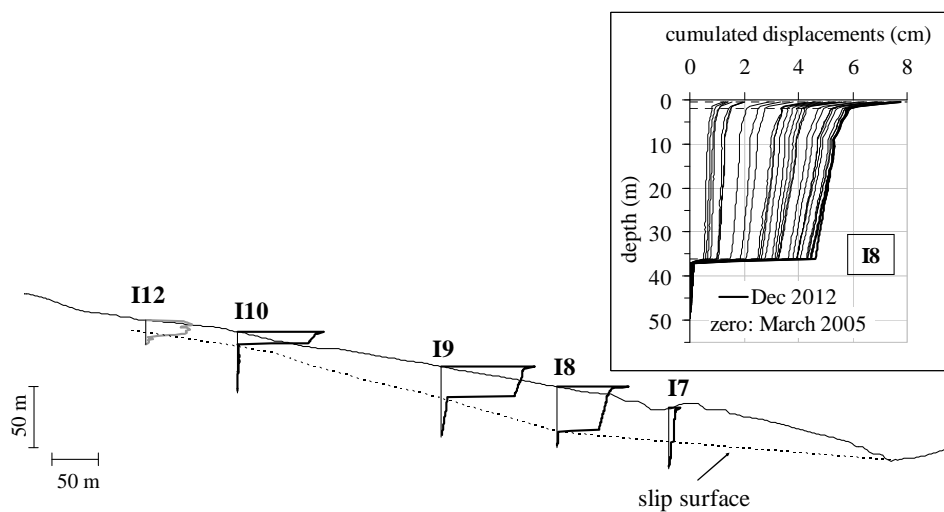


Fig. 2. Longitudinal median section of the earthflow with inclinometer profiles.

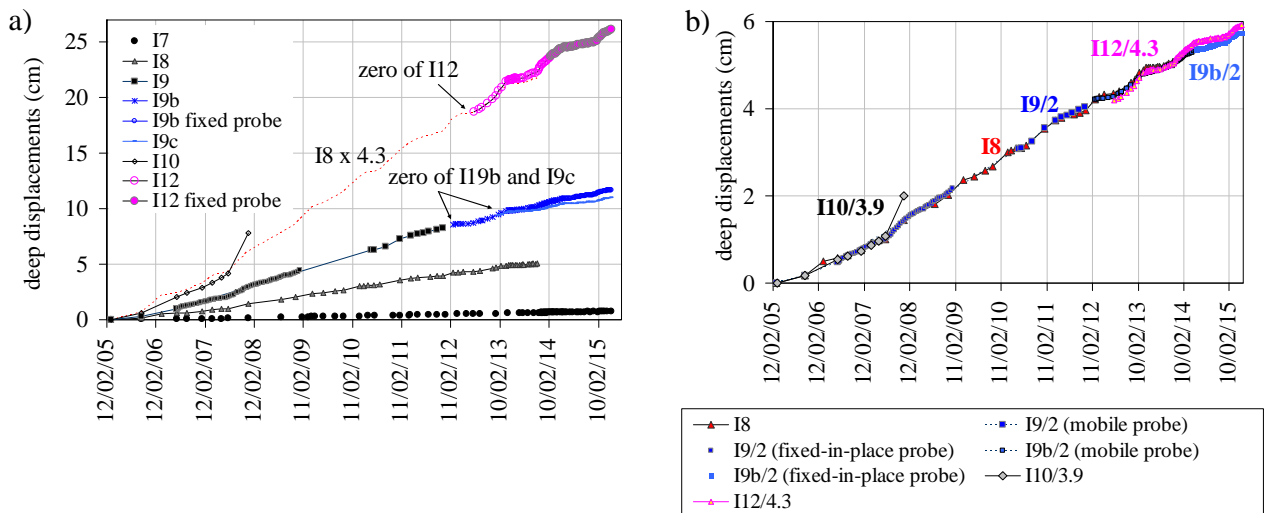


Fig. 3. Relative displacements on the slip surface against time: a) measured; b) scaled with reference to I8 time-trend (update of the results reported by Di Maio et al. 2013).

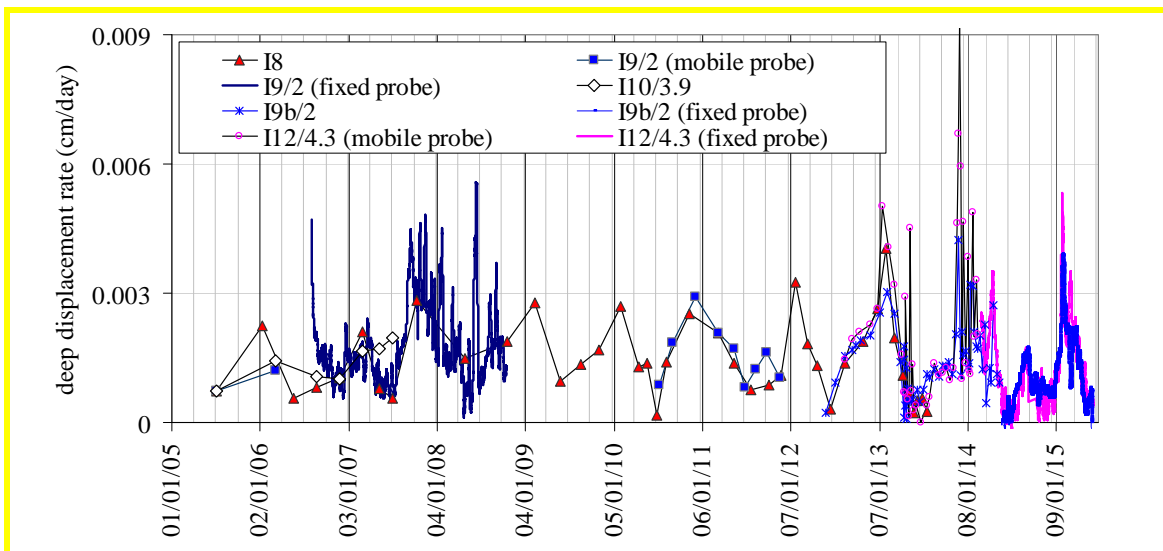


Fig. 4. Displacement rate on the shear surface obtained from fixed-in-place inclinometer measurements by using 15 days moving average and from mobile inclinometer measurements. Data series of every inclinometer was scaled with reference to I8 time-trend.

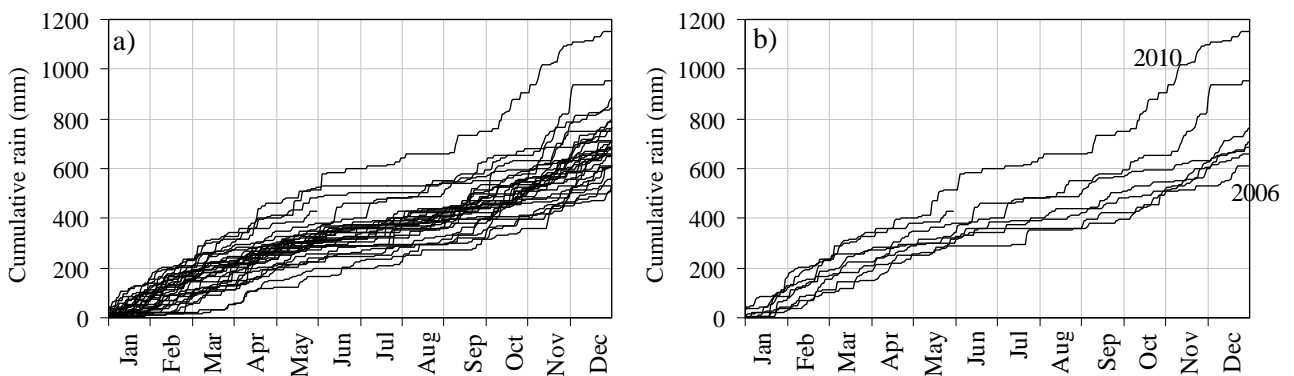


Fig. 5. Cumulative rainfall series: a) over years 1980-2015; b) over the period of monitoring, 2005-2015.

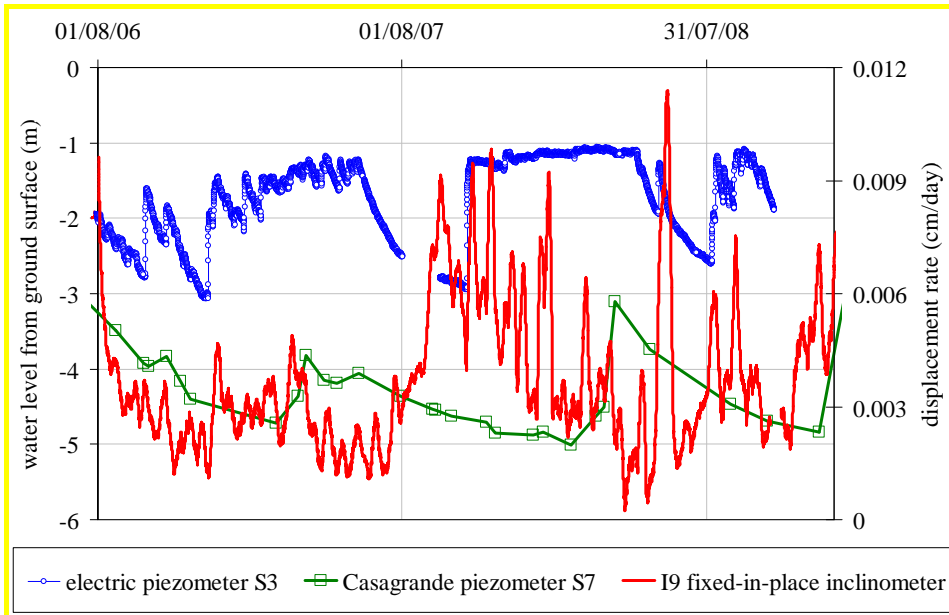


Fig. 6: Comparison of the time trends of displacement rates measured in inclinometer I9 and of water level from the ground surface measured in piezometers S3 and S7.

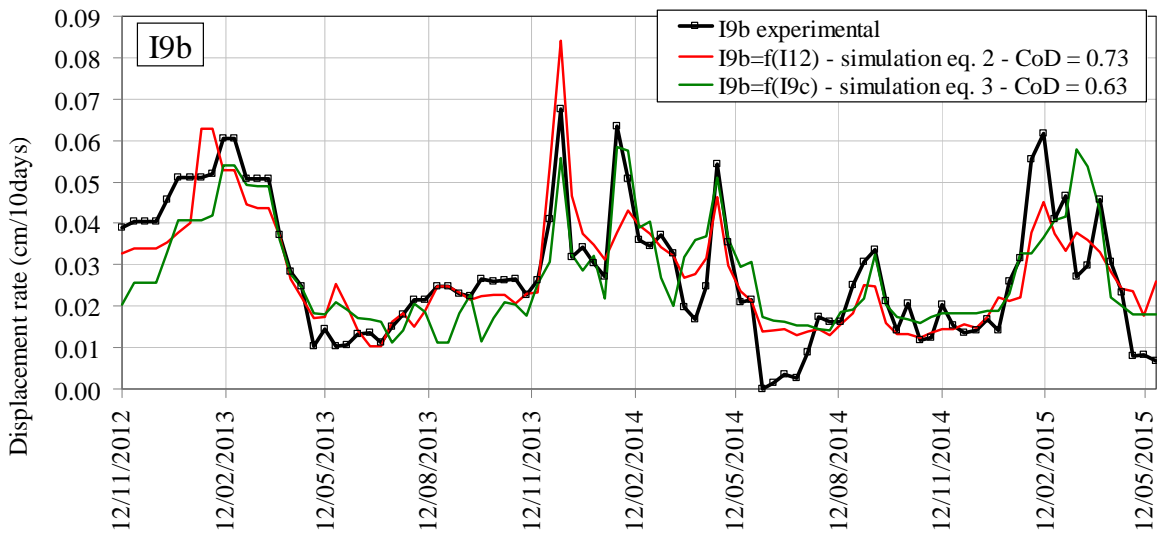


Fig. 7: Time plot of displacement rates measured in situ in I9b and calculated by equation (2), I9b vs. I12, and (3), I9b vs. I9c.

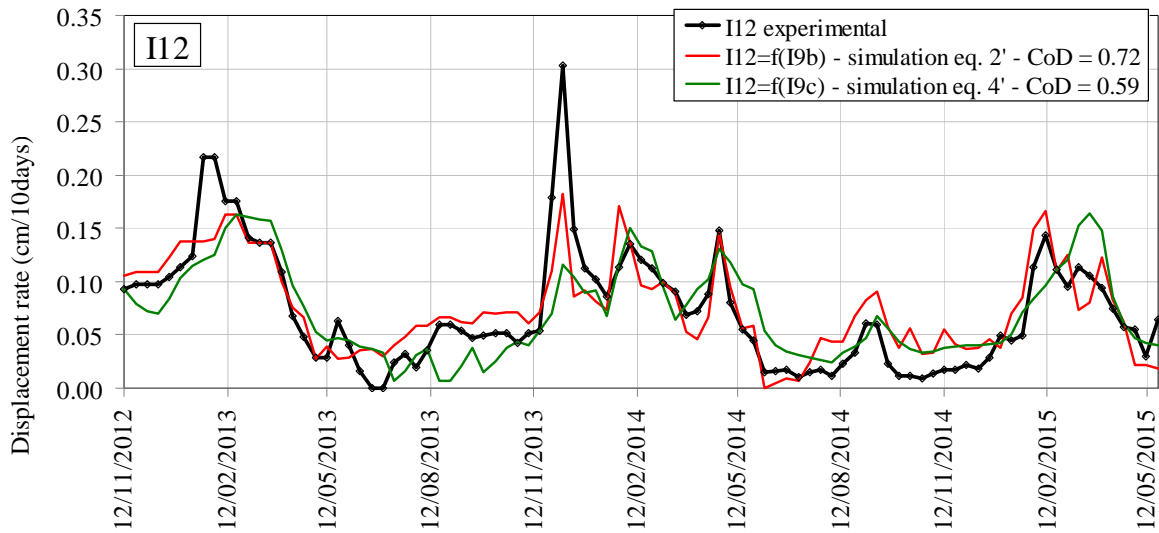


Fig. 8: Time plot of displacement rates measured in situ in I12 and calculated by equation (2'), I12 vs. I9b, and (4'), I12 vs. I9c.

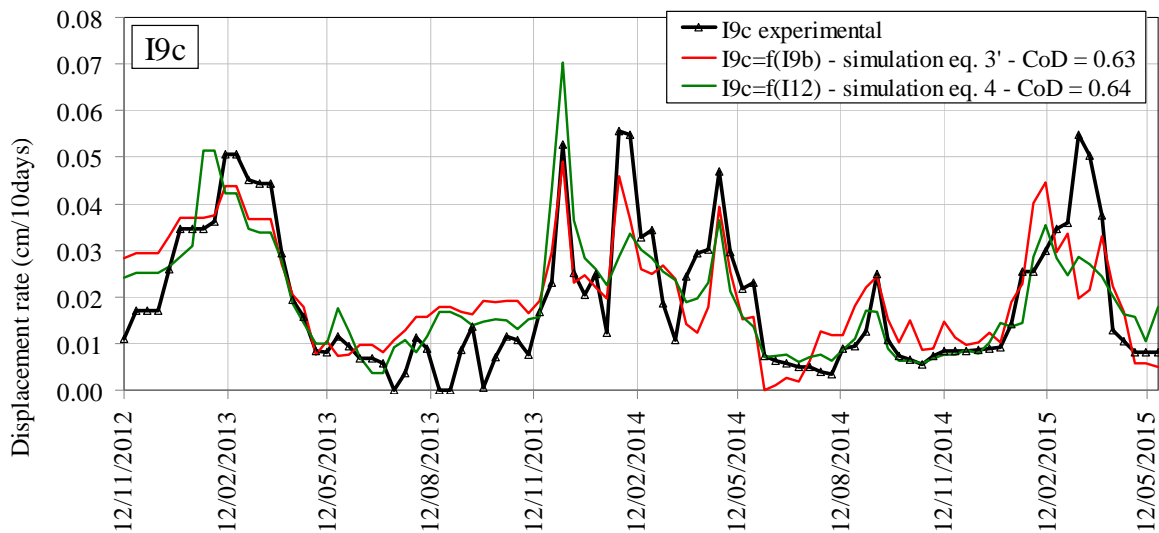


Fig. 9: Time plot of displacement rates measured in situ in I9c and calculated by equation (3'), I9c vs. I9b, and (4), I9c vs. I12.

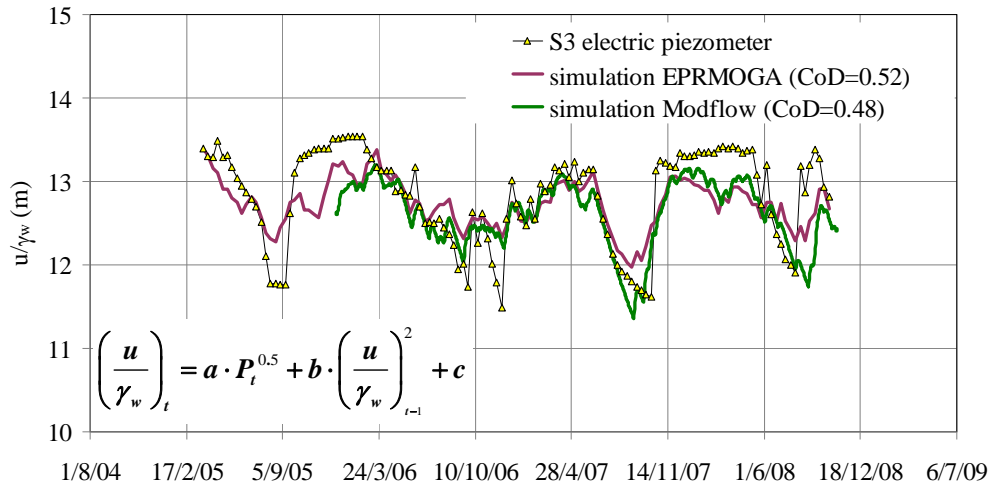


Fig. 10: Time plots of pressure head u/γ_w measured by electric piezometer S3, calculated by equation (5), and obtained through the Modflow 3D transient simulation by Vassallo et al. (2014).

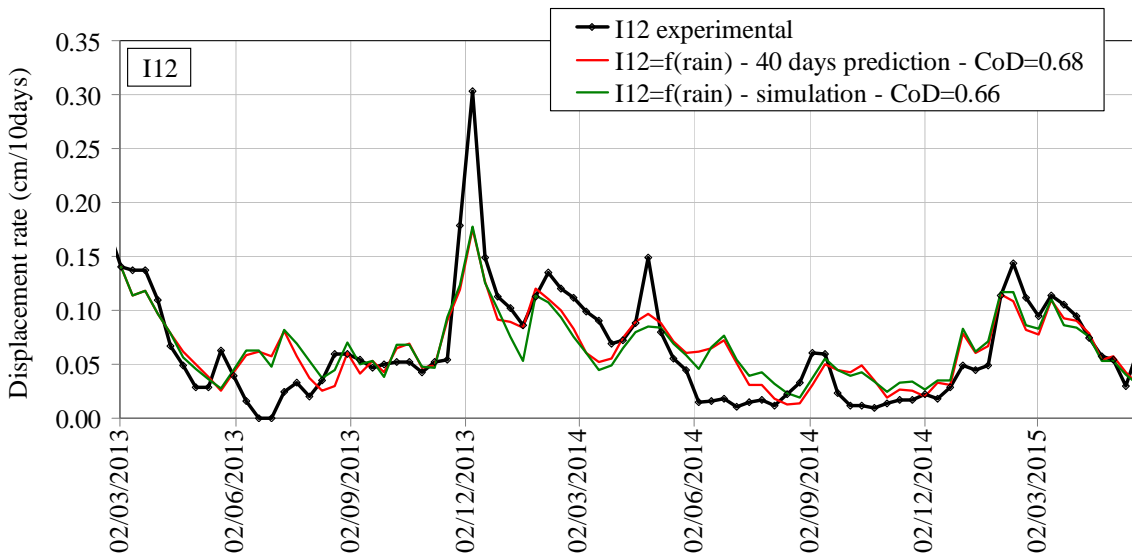


Fig. 11: Time plot of displacement rates of I12: measured data, 40-days ahead prediction and simulation obtained by equation (6).

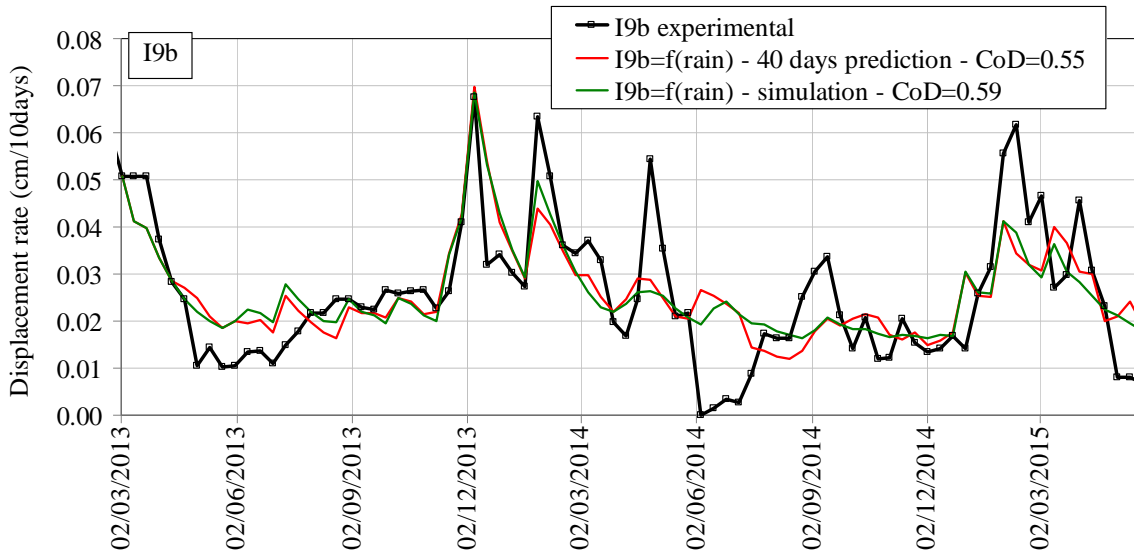


Fig. 12: Time plot of displacement rates of I9b: measured data, 40-days ahead prediction and simulation obtained by equation (7).

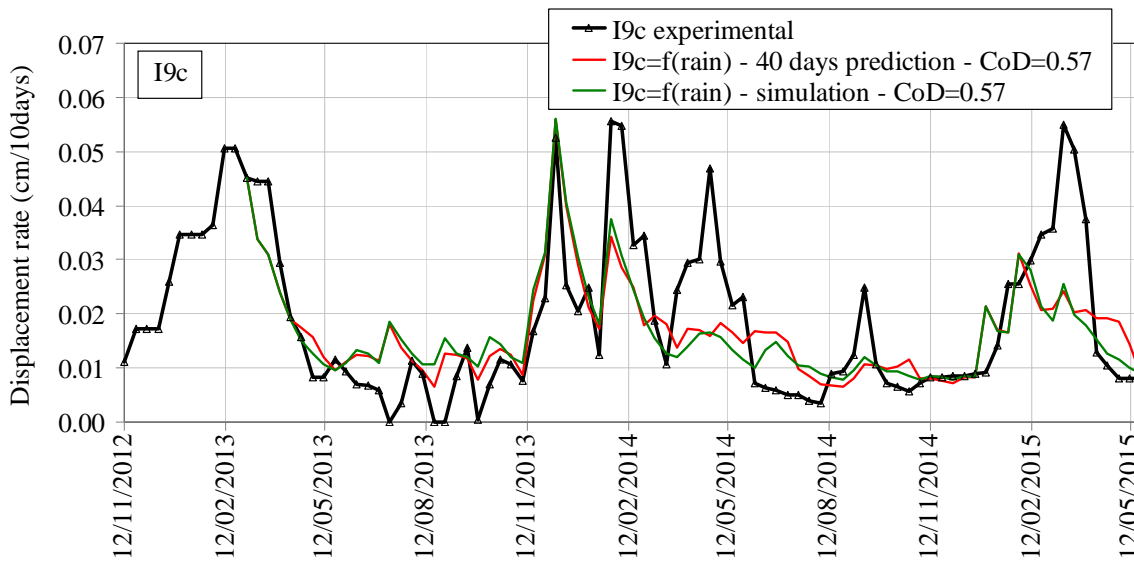


Fig. 13: Time plot of displacement rates of I9c: measured data, 40-days ahead prediction and simulation obtained by equation (8).

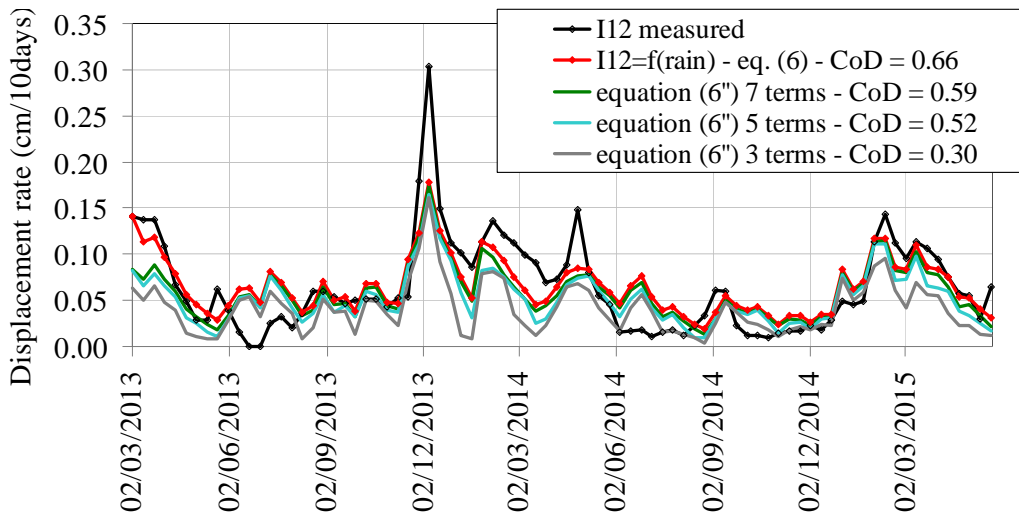


Fig. 14: Time plot of displacement rates measured in I12 compared to those obtained by equation (6) and by equation (6'') considering all its seven terms or just the first 5 or the first 3.

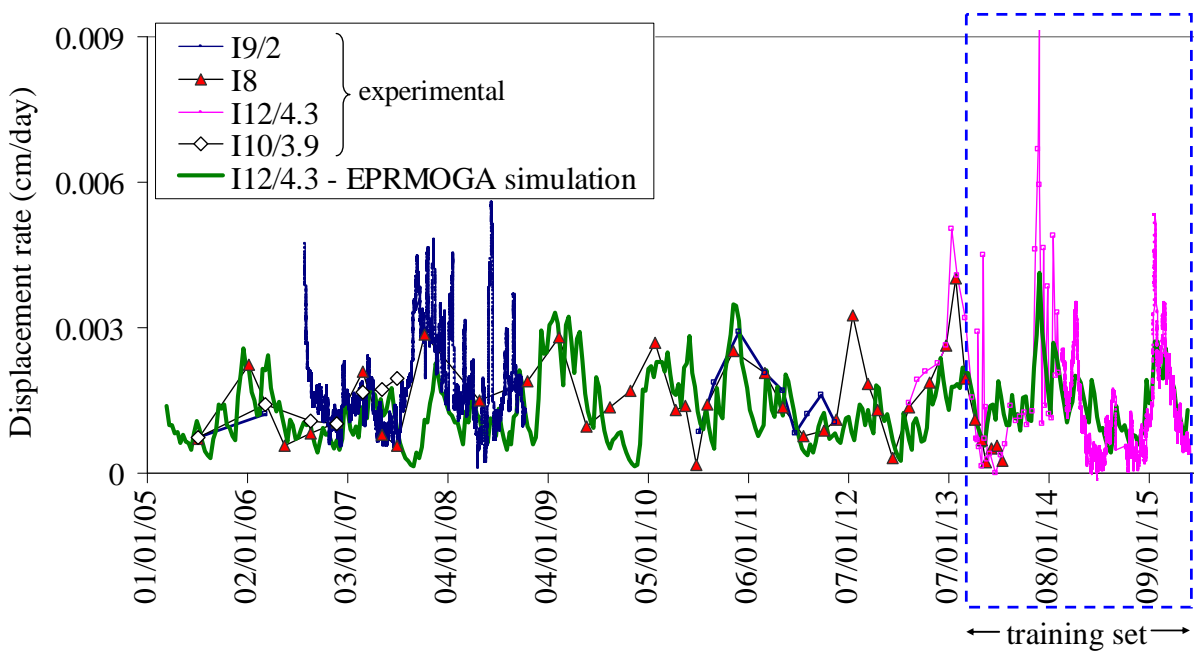


Fig. 15: Comparison between EPRMOGA simulation over the whole monitoring period 2005-2015 and measured displacement rates in different points of the landslide. The simulation was calibrated on the experimental data of inclinometer I12 in the period 2013-2015.